

CO Oxidation Over Ceria-Based Catalysts: Comparison of Single and Binary Metal Oxides

Marco Piumetti*, Samir Bensaid, Tahrizi Andana, Melodj Dosa, Nunzio Russo, Raffaele Pirone and Debora Fino

Department of Applied Science and Technology, Politecnico di Torino, Corso Duca degli Abruzzi 24, 10129 Torino, Italy

Abstract: A set of single metal oxides (CeO_2 , ZrO_2 , PrO_2 , CuO and Fe_2O_3) and binary oxide catalysts ($\text{Ce}_{80}\text{Zr}_{20}$, $\text{Ce}_{80}\text{Pr}_{20}$, $\text{Ce}_{80}\text{Cu}_{20}$ and $\text{Ce}_{80}\text{Fe}_{20}$) prepared by the solution combustion synthesis was tested for the CO oxidation reaction. As a whole, the best catalytic activity was achieved for the $\text{Ce}_{80}\text{Cu}_{20}$ catalyst (binary oxide with Ce = 80 at.% and Cu = 20 at.%). This confirms that CeO_x and CuO_x phases may cooperate effectively for this oxidation process. The easier surface reducibility of this catalyst should promote the CO oxidation reaction. Likewise, it appears that the presence of metals, such as the Cu, Zr, Fe and Pr, into the ceria framework has a beneficial effect on the CO oxidation via cooperative phenomena among the redox active centres. All the prepared catalysts were characterized by the powder XRD, FE-SEM, N_2 physisorption at -196°C and H_2 -TPR analysis.

Keywords: CO oxidation, Ceria, Solution combustion synthesis, Cooperative phenomena, Oxidation catalysis.

1. INTRODUCTION

Every year, large amounts of CO are emitted in the world, mainly from transportation, power plants, industrial and domestic activities. Therefore, it is necessary to limit the CO emissions and develop new technologies to convert CO into valuable compounds. In this scenario, the growing petrochemical industry has resulted in the removal of CO from large gas streams and noble metals have been used to oxidize CO at low temperature. In fact, CO oxidation over noble metal based catalysts takes place in car exhaust after treatment systems, especially for gasoline engines since oxygen-deficient regions occur [1-3]. CO oxidation over solids represents the simplest heterogeneously catalyzed reaction and it can thus be considered as a prototypical reaction for heterogeneous processes. In other words, CO oxidation can be used as a suitable model reaction for more complex catalytic oxidation processes and for studying the nature of active sites [4, 5]. According to the literature, effective solid catalysts for the CO oxidation are found in the Group VIII metals. As a whole, noble metals are more active, but more expensive than base metals. Thus, several metal oxides (especially ceria-based materials) have been investigated and it has been observed that they may exhibit interesting activity for the CO oxidation [4-7]. Moreover

, it has been verified that the incorporation of metals (e.g. Fe, Cu, Zr, Pr) into the CeO_2 lattice may have a beneficial effect on the structural and electronic properties of the catalyst, thus improving their oxidation activity and thermal stability [7-9]. In heterogeneous catalysis, in fact, there are several characteristic examples in which the presence of multi-component catalysts influences the solid-state chemistry, since active phases (and promoters) may interact with each other [10-12]. In the present work, a set of single metal oxides (namely, CeO_2 , ZrO_2 , PrO_2 , CuO and Fe_2O_3) and binary oxide catalysts ($\text{Ce}_{80}\text{Zr}_{20}$, $\text{Ce}_{80}\text{Pr}_{20}$, $\text{Ce}_{80}\text{Cu}_{20}$ and $\text{Ce}_{80}\text{Fe}_{20}$) was synthesized by the solution combustion synthesis (SCS) and their catalytic activity was tested for the CO oxidation. Then, the catalysts were characterized by complementary techniques, such as the powder XRD, FESEM, N_2 physisorption at -196°C and H_2 -TPR.

2. MATERIALS AND METHODS

2.1. Catalysts Preparation

A set of single metal oxides (CeO_2 , ZrO_2 , PrO_2 , CuO and Fe_2O_3) and binary oxide catalysts ($\text{Ce}_{80}\text{Zr}_{20}$, $\text{Ce}_{80}\text{Pr}_{20}$, $\text{Ce}_{80}\text{Cu}_{20}$ and $\text{Ce}_{80}\text{Fe}_{20}$, where the numbers indicate the atomic %) was synthesized by means of solution combustion synthesis (SCS) [13, 14]. In short, for the preparation of binary oxide catalysts, 0.8 g of urea and 1.9 g of a stoichiometric mixture (80:20) of $\text{Ce}(\text{NO}_3)_3 \cdot 6\text{H}_2\text{O}$ and one of these following metal salt precursors: $\text{Zr}(\text{NO}_3)_2$, $\text{Pr}(\text{NO}_3)_3$, $\text{Cu}(\text{NO}_3)_2$ and $\text{Fe}(\text{NO}_3)_3$, were dissolved in 50 ml of deionized

*Address correspondence to this author at the Department of Applied Science and Technology, Politecnico di Torino, Corso Duca degli Abruzzi 24, 10129 Torino, Italy; Tel: +39-011-0904753; Fax: +39-011-0904699; E-mail: marco.piumetti@polito.it

water and stirred at room temperature (r.t.) for 30 min. The homogeneous solution was then placed in oven at 600 °C for 20 min. Single metal oxide catalysts were prepared with the same procedure with the corresponding precursor (metal nitrate).

2.2. Catalyst Characterization

The X-ray diffraction patterns were collected on an X' Pert Philips PW3040 diffractometer using Cu K α radiation (2θ range = 15°– 70°; step = 0.05° 2θ ; time per step = 0.2 s). The XRD patterns were indexed according to the Powder Data File database (PDF 2000, International Centre of Diffraction Data, Pennsylvania). Sample morphology was observed through a field emission scanning electron microscope (FESEM Zeiss MERLIN, Gemini-II column). The specific surface area (SSA) and total pore volume (V_p) were measured by N $_2$ physisorption at -196 °C (Micrometrics ASAP 2020) on powders previously out gassed at 200 °C for 4 h to remove water and other atmospheric contaminants; SSA was determined according to the Brunauer-Emmett-Teller (BET) method. H $_2$ -TPR analysis was performed to study the catalyst reducibility. Sample pretreatment was conducted prior to analysis by treating 50 mg of catalyst under air (40 ml min $^{-1}$) at 150 °C for 1 h, followed by cooling with Ar to r.t. H $_2$ -TPR analysis was executed by increasing gradually sample temperature to 750 °C with the rate of 5°C min $^{-1}$ under Ar (4.95 %mol H $_2$ in Ar). The instrument was equipped with thermal conductivity detector (TCD) to recognize the H $_2$ signal.

2.3. Catalytic Activity Tests

Catalytic activity tests were performed in a quartz U-tube reactor with inner diameter = 4 mm, heated by an electric furnace; the temperature was measured by means of a thermocouple placed in the middle of the catalytic bed. In a typical run, 0.1 g of powdered catalyst was inserted in the reactor. Then, the catalytic bed was pre-treated in He (flow rate = 50 ml min $^{-1}$) for 1 h at 150 °C. The test started by flowing 50 ml min $^{-1}$ gas containing 1000 ppm of CO and 10% O $_2$ in N $_2$ into the reactor (GHSV of 19100 h $^{-1}$). The temperature was then raised by 5 °C min $^{-1}$ in the 50–450 °C temperature range. The CO and CO $_2$ concentrations at the outlet of the reactor were measured by NDIR analyzers (ABB Uras 14). Temperatures at which 10, 50, and 90 % of CO was converted were taken as indices of the catalytic activity ($T_{10\%}$, $T_{50\%}$ and $T_{90\%}$, respectively). The

tests were conducted for 2 cycles to evaluate the stability of the catalysts.

3. RESULTS AND DISCUSSION

Figure 1 shows the X-ray diffractograms of the pure ceria and ceria-based materials. The binary oxide catalysts (Ce $_{80}$ Zr $_{20}$, Ce $_{80}$ Pr $_{20}$, Ce $_{80}$ Cu $_{20}$ and Ce $_{80}$ Fe $_{20}$) refer to a cubic fluorite structure of ceria, indicated by (111), (200), (220), (311), and (222) peaks [15, 16]. No additional peaks due to ZrO $_2$, PrO $_2$, CuO or Fe $_2$ O $_3$ phases, respectively, were found in the diffractograms, thus confirming the presence of a single phase for these materials.

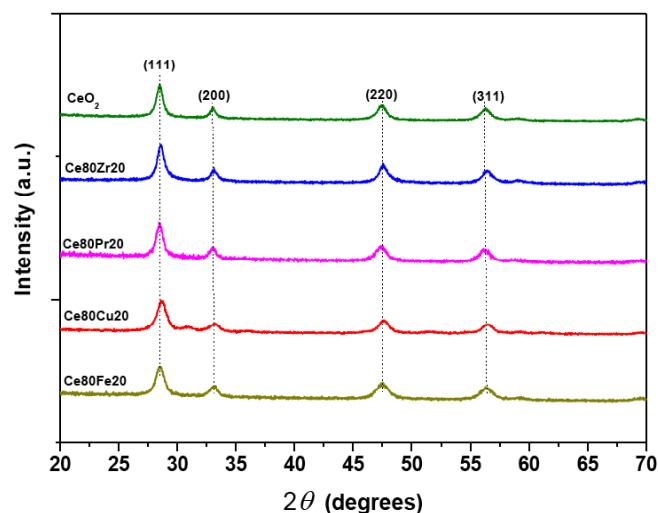


Figure 1: X-ray diffractograms of the ceria-based catalysts.

The BET specific surface area and total pore volume of the samples, derived from N $_2$ physisorption, are resumed in Table 1. As a whole, the addition of foreign metals generally improves the textural

Table 1: Textural Properties of the Prepared Catalysts

| Sample | SSA m 2 g $^{-1}$ | V_p cm 3 g $^{-1}$ |
|-----------------------|-------------------------|----------------------------|
| CeO $_2$ | 15 | 0.02 |
| ZrO $_2$ | 1 | 0.01 |
| PrO $_2$ | 9 | 0.03 |
| CuO | 1 | 0.01 |
| Fe $_2$ O $_3$ | 17 | 0.03 |
| Ce $_{80}$ Zr $_{20}$ | 23 | 0.04 |
| Ce $_{80}$ Pr $_{20}$ | 16 | 0.03 |
| Ce $_{80}$ Cu $_{20}$ | 18 | 0.03 |
| Ce $_{80}$ Fe $_{20}$ | 19 | 0.03 |

properties by increasing surface areas, as compared to pure ceria; however, the increment depends much on the nature of metals. Specifically, Zr, Fe and Cu species into the ceria enlarges the surface area in the 16-23 m²g⁻¹ range, as follows:

$$\text{Ce100} \approx \text{Ce80Pr20} < \text{Ce80Cu20} \approx \text{Ce80Fe20} < \text{Ce80Zr20}$$

On the other hand, embedding the Pr species into ceria does not significantly modify the textural features. This finding might be because both cerium and praseodymium ions are nearly identical in size.

Figure 2 shows the morphology for all the catalysts observed through the FESEM. As expected, different shapes can be observed for the CeO₂, ZrO₂, PrO₂, CuO and Fe₂O₃ samples. Briefly, spongy frameworks (agglomerated) occur for both the CeO₂ and Fe₂O₃, at variance of the PrO₂ and CuO samples, in which relatively large lamellar systems occur. On the other hand, small spherical particles (in the 10-20 nm range) can be observed for the ZrO₂ sample. All the binary oxides prepared by the solution combustion technique exhibit a spongy ceria-like framework (three-dimensional shapes) comprising of small nanoscale agglomerates. The presence of various foreign metals into the ceria lattice, indeed, does not significantly affect the ceria morphology.

Figure 3 shows the H₂-TPR curves for the prepared catalysts. Pure CeO₂ exhibits a wide peak centred at 475 °C due to the surface reduction of ceria [17, 18], while the reduction of bulk CeO₂ occurs above 900 °C. Indeed, the low-temperature reduction peak infers the role of surface oxygens, which are weakly attached to

the solid surface; the final reduction is eventually triggered by the release of lattice oxygens at high temperature. A similar trend appears for the ZrO₂ sample. The PrO₂ sample has two reduction peaks centred at 407 and 495 °C, whereas the CuO and Fe₂O₃ samples exhibit the main reduction in the 380-420 °C temperature range. Among the binary oxide catalysts, the following increasing reducibility scale can be drawn:

$$\text{Ce80Zr20} < \text{Ce80Pr20} < \text{Ce80Fe20} < \text{Ce80Cu20}$$

The Ce80Cu20 sample appears the most reducible catalyst, having two peaks centred at 185 and 250 °C, corresponding to CuO_x clusters strongly interacting with CeO₂. In other words, the co-presence of CeO_x and CuO_x species may promote the surface reducibility and then the redox activity [18-21]. A similar trend, although with less extent, can be observed for the Ce80Fe20 and Ce80Pr20 samples, showing reduction peaks centred at 375 °C and in the 405-490 °C range, respectively. Although the temperature for the main reduction peak of ceria-praseodymia sample is higher than that of pure ceria, the reduction of Ce80Pr20 commences at lower temperature. This finding suggests that praseodymium favors the weakening of Ce-O bonds, as observed in our previous work [22]. On the other hand, higher reduction temperatures appear for the Ce80Zr20 sample, thus confirming the role of Zr⁴⁺ cations on the reduction resistance of ceria [23].

Figure 4 shows the CO conversion to CO₂ (%) as a function of the temperature for the single metal oxides (dotted curves) and binary oxide catalysts (bold curves), along with the uncatalyzed reaction (black curve). As a whole, all the oxide catalysts improve

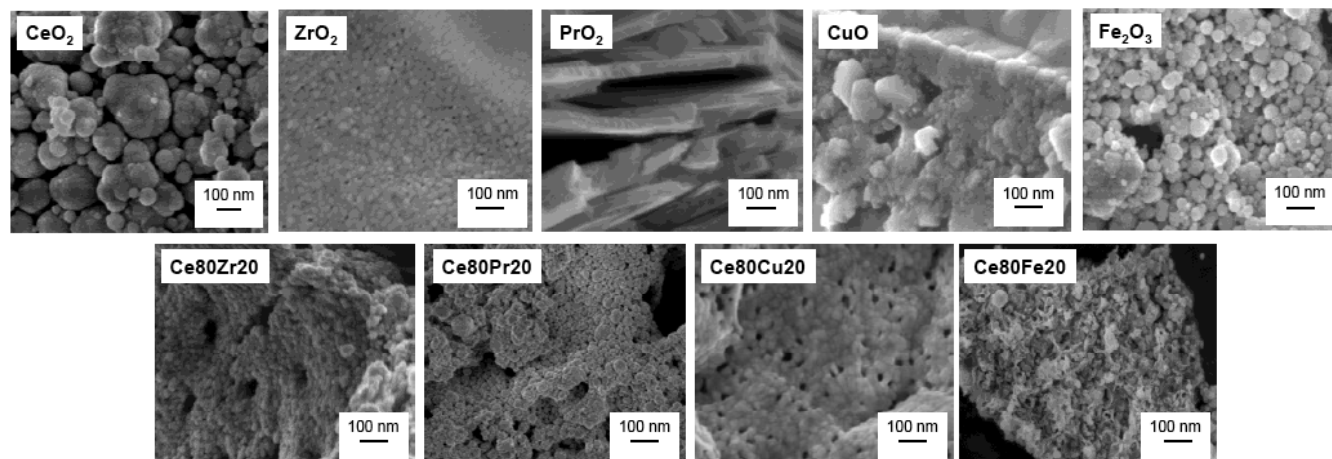


Figure 2: FESEM images of the prepared catalysts.

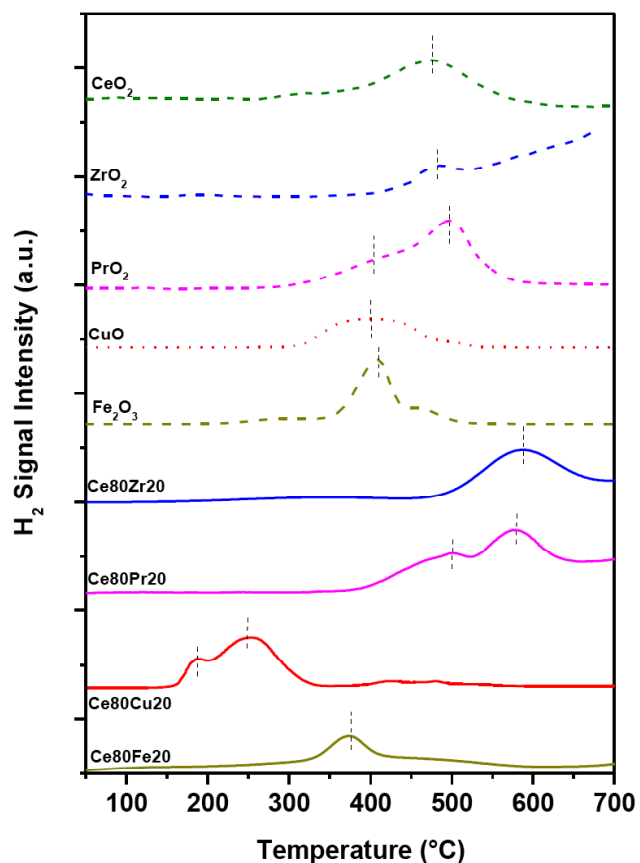
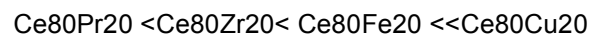


Figure 3: H₂-TPR profiles of the prepared samples.

greatly the CO conversion, where as $\approx 30\%$ of CO converts thermally to CO₂ at 450 °C. For the single metal oxides, the following increasing oxidation activity order (measured in terms of T_{10%} and T_{50%}) can be designed:



and for the binary oxide catalysts, the increasing order is:



For both sets of catalysts, the activity trends are in fair agreement with the H₂-TPR data (*vide supra*), thus confirming that the catalyst reducibility has a beneficial effect on the CO oxidation. In fact, the more reducible the catalyst surface, the easier the release of surface oxygen accessible to CO molecules. On the other hand, high electronic conductivity and oxygen anion mobility are beneficial factors for the oxidation process [10, 24]. Figure 5 shows the catalyst activities (measured in terms of T_{10%}, T_{50%} and T_{90%}) by means of the Venn diagrams. As a whole, it appears that the presence of metals such as the Cu, Zr, Fe and Pr in the ceria framework has a beneficial effect on the CO oxidation, as compared to pure ceria. However, the cooperation among the ceria and foreign metal oxides seems effective with transition metals rather than with praseodymium, since PrO₂ appears more active than CeO₂ and Ce80Pr20. The cooperation between ceria and foreign metal oxides is particularly marked for the Ce80Cu20 sample, thus rendering the latter material particularly interesting for oxidation applications.

CONCLUSIONS

In the present paper, we studied single metal oxides (CeO₂, ZrO₂, PrO₂, CuO and Fe₂O₃) and binary oxide catalysts (Ce80Zr20, Ce80Pr20, Ce80Cu20 and

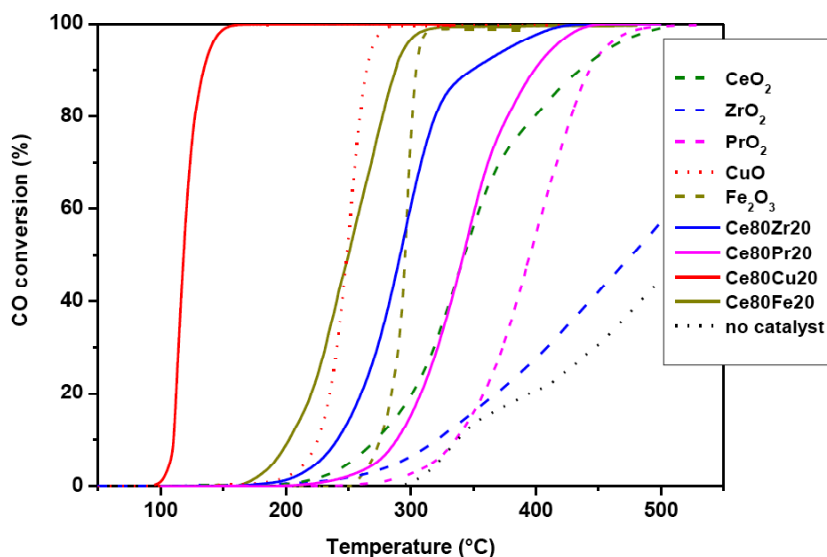


Figure 4: CO oxidation profiles as a function of temperature for the prepared catalysts (GHSV = 19100 h⁻¹)

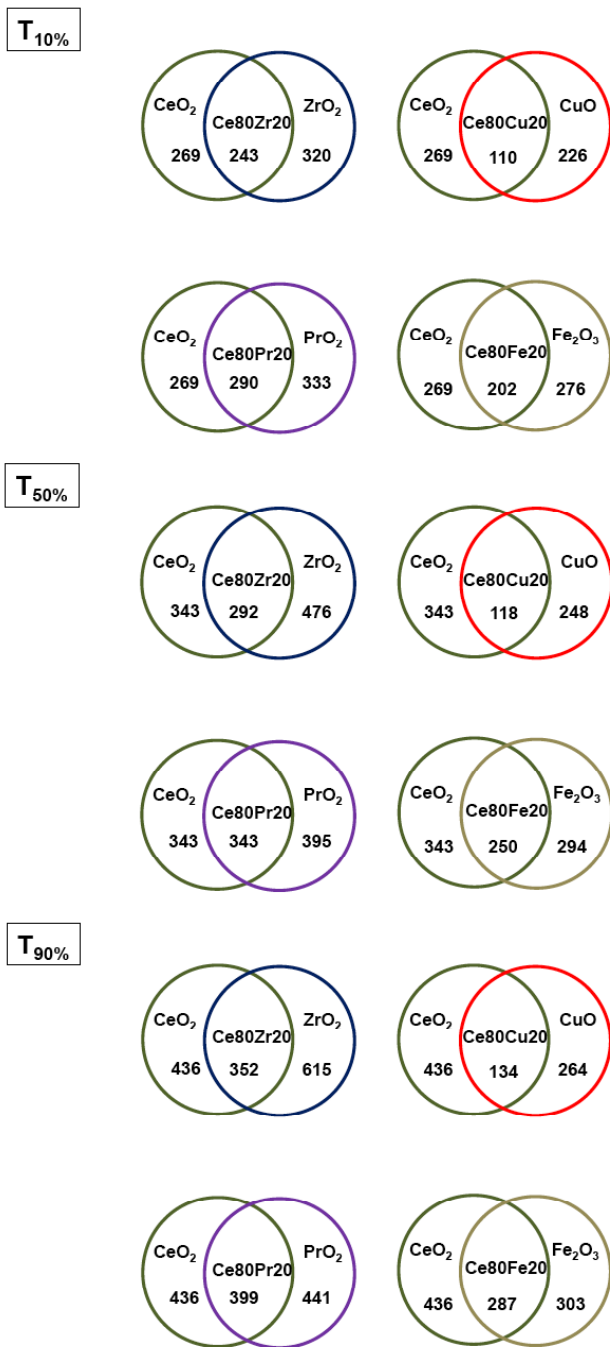
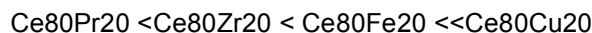


Figure 5: Venn diagrams of the catalytic performances (in terms of $T_{10\%}$, $T_{50\%}$ and $T_{90\%}$) achieved for the prepared catalysts.

Ce80Fe20) prepared by the solution combustion synthesis, effective for the CO oxidation. For the single metal oxides, the increasing catalyst activity order (measured in terms of $T_{10\%}$ and $T_{50\%}$) was:



where as for the binary oxide catalysts, the increasing activity order was:



For both sets of catalysts, the activity trends are in fair agreement with the H_2 -TPR data, thus confirming that the catalyst reducibility has a beneficial effect towards the CO oxidation reaction. These results confirm that the presence of metals such as the Cu, Zr, Fe or Pr in the ceria framework may promotes the CO oxidation reaction via cooperative phenomena among the redox active centres. The cooperation between ceria and foreign metal oxides is particularly marked for the Ce80Cu20, thus rendering the latter catalytic material particularly interesting for future investigations in the field of oxidation catalysis.

ACKNOWLEDGMENTS

The Ministero dell'Università e della Ricerca (MIUR) (grant number: RBFR12LS6M 001) is acknowledged for sponsoring this research activity (FIRB - Futuro in Ricerca 2012).

REFERENCES

- [1] Ertl G, Knözinger H, Schüth F, Weitkamp J. "Handbook of Heterogeneous Catalysis" (2nd ed.), Wiley-VCH, Weinheim, 2008.
<http://dx.doi.org/10.1002/9783527610044>
- [2] Hodnett BK. "Heterogeneous Catalytic Oxidation", Wiley-VCH, New York, 2000.
- [3] Freund HJ, Meijer G, Scheffler M, Schögl R, Wolf M. "CO Oxidation as a Prototypical Reaction for Heterogeneous Processes", *Angew Chem Int Ed* 2011; 50: 10064-10094.
<http://dx.doi.org/10.1002/anie.201101378>
- [4] Royer S, Duprez D. "Catalytic Oxidation of Carbon Monoxide over Transition Metal Oxides", *Chem Cat Chem* 2011; 3: 24-65.
<http://dx.doi.org/10.1002/cctc.201000378>
- [5] Wu ZL, Li MJ, Overbury SH. "On the structure dependence of CO oxidation over CeO₂ nanocrystals with well-defined surface planes", *J Catal* 2012; 285: 61-73.
<http://dx.doi.org/10.1016/j.jcat.2011.09.011>
- [6] Russo N, Fino D, Saracco G, Specchia V. "Supported gold catalysts for the CO oxidation", *Catal Today* 2006; 117: 214-219.
<http://dx.doi.org/10.1016/j.cattod.2006.05.027>
- [7] Piumetti M, Bensaid S, Fino D, Russo N. "Nanostructured ceria-zirconia catalysts for the CO oxidation: Study on surface properties and reactivity", *Appl Catal B* 2016; 197: 35-46.
<http://dx.doi.org/10.1016/j.apcatb.2016.02.023>
- [8] Trovarelli A, Fornasiero P. "Catalysis by Ceria and Related Materials" 2nd ed., Imperial College Press, London, 2013.
<http://dx.doi.org/10.1142/p870>
- [9] Bueno-López A. "Diesel soot combustion ceria catalysts", *Appl Catal B* 2014; 146: 1-11.
<http://dx.doi.org/10.1016/j.apcatb.2013.02.033>
- [10] Vedrine JC, *Appl. Catal.* "A Revisiting active sites in heterogeneous catalysis: Their structure and their dynamic behaviour" 2014; 274, 40-50.
- [11] Van Santen RA, Neurock M. "Molecular Heterogeneous Catalysis", Wiley-VCH, Verlag 2006; 61-62

- [12] Carson G, Coudurier JC, Védrine A, Laarif F, Theobald J. "Synergy effects in the catalytic properties of bismuth molybdates", *J Chem Soc Faraday Trans I* 1983; 79: 1921-1929.
<http://dx.doi.org/10.1039/f19837901921>
- [13] González-Cortés SL, Imbert FE. "Fundamentals, properties and applications of solid catalysts prepared by solution combustion synthesis (SCS)", *Appl Catal A* 2013; 452: 117-131.
<http://dx.doi.org/10.1016/j.apcata.2012.11.024>
- [14] Civera A, Pavese M, Saracco G, Specchia V. "Combustion synthesis of perovskite-type catalysts for natural gas combustion", *Catal Today* 2003; 83: 199-211.
[http://dx.doi.org/10.1016/S0920-5861\(03\)00220-7](http://dx.doi.org/10.1016/S0920-5861(03)00220-7)
- [15] Thrimurthulu G, Rao KN, Devaiah D, Reddy BM "Nanocrystalline ceriapraseodymia and ceria-zirconia solid solutions for soot oxidation" *Res Chem Intermed* 2012; 38:1847-1855
<http://dx.doi.org/10.1007/s11164-012-0508-y>
- [16] Reddy BM, Thrimurthulu G, Katta L, Yamada Y, Park SE. "Structural characteristics and catalytic activity of nanocrystalline ceria-praseodymia solid solutions", *J Phys Chem C* 2009; 113: 15882-15890.
<http://dx.doi.org/10.1021/jp903644y>
- [17] Piumetti M, Bensaid S, Russo R, Fino D. "Nanostructured ceria-based catalysts for soot combustion: Investigations on the surface sensitivity", *Appl Catal B* 2015; 165: 742-751
<http://dx.doi.org/10.1016/j.apcatb.2014.10.062>
- [18] Caputo T, Lisi L, Pirone R, Russo N. "On the role of redox properties of CuO/CeO₂ catalysts in the preferential oxidation of CO in H₂-rich gases", *Appl Catal A* 2008; 348: 42-53.
<http://dx.doi.org/10.1016/j.apcata.2008.06.025>
- [19] Avgouropoulos G, Ioannides T. "Selective CO oxidation over CuO-CeO₂ catalysts prepared via the urea-nitrate combustion method", *Appl Catal A* 2003; 244: 155-167.
[http://dx.doi.org/10.1016/S0926-860X\(02\)00558-6](http://dx.doi.org/10.1016/S0926-860X(02)00558-6)
- [20] Delimaris D, Ioannides T. "VOC oxidation over CuO-CeO₂ catalysts prepared by a combustion method" *Appl Catal B* 2009; 89: 295-302.
<http://dx.doi.org/10.1016/j.apcatb.2009.02.003>
- [21] Heynderickx PM, Thybaut JW, Poelman H, Poelman D, Marin GB. "The total oxidation of propane over supported Cu and Ce oxides: A comparison of single and binary metal oxides", *J Catal* 2010; 272: 109-120.
<http://dx.doi.org/10.1016/j.jcat.2010.03.006>
- [22] Andana T, Piumetti M, Bensaid S, Russo N, Fino D, Pirone R. "Nanostructured ceria-praseodymia catalysts for diesel soot combustion", *Appl Catal B* 2016; 197: 125-137.
<http://dx.doi.org/10.1016/j.apcatb.2015.12.030>
- [23] Piumetti M, Bensaid S, Russo N, Fino D. "Investigations into nanostructured ceria-zirconia catalysts for soot combustion", *Appl Catal B* 2016; 180: 271-282.
<http://dx.doi.org/10.1016/j.apcatb.2015.06.018>
- [24] Grasselli RK. "Genesis of site isolation and phase cooperation in selective oxidation catalysis" *Top Catal* 2001; 15: 93-101.
<http://dx.doi.org/10.1023/A:1016683117255>

Received on 03-10-2016

Accepted on 13-10-2016

Published on 27-10-2016

<http://dx.doi.org/10.15379/2408-9834.2016.03.02.01>

© 2016 Piumetti et al.; Licensee Cosmos Scholars Publishing House.

This is an open access article licensed under the terms of the Creative Commons Attribution Non-Commercial License (<http://creativecommons.org/licenses/by-nc/3.0/>), which permits unrestricted, non-commercial use, distribution and reproduction in any medium, provided the work is properly cited.